Analysis of the T-point-Hopf bifurcation with $\mathbb{Z}_2$-symmetry. Application to Chua's equation

Antonio Algaba[†], Fernando Fernández-Sánchez[‡],

Manuel Merino[†], Alejandro J. Rodríguez-Luis[‡].

† Dept. Mathematics
Facultad de Ciencias Experimentales, Univ. Huelva
Avda. Tres de Marzo s/n
21071 Huelva
Spain

‡ Dept. Applied Mathematics II
E.S. Ingenieros, Univ. Sevilla
Camino de los Descubrimientos s/n
41092 Sevilla
Spain

July 27, 2009

Abstract

The aim of this work is twofold. On the one hand, to perform a theoretical analysis of the global behavior organized by a T–point–Hopf in $\mathbb{Z}_2$-symmetric systems. On the other hand, to apply the obtained results for a numerical study of Chua's equation, where it is the first time this bifurcation is considered.

In a parameterized three–dimensional system of autonomous differential equations, a T–point is a point of the parameter space where a special kind of codimension–two heteroclinic cycle occurs. A more degenerate scenario appears when one of the equilibria involved in such a cycle undergoes a Hopf bifurcation. This degeneration, which corresponds to a codimension–three bifurcation, is

called T–point–Hopf and has been recently studied for a generic system. However, the presence of $\mathbb{Z}_2$-symmetry may lead to the existence of a double T–point–Hopf heteroclinic cycle, which is responsible for the appearance of interesting global behavior that we will study in this paper.

The theoretical models proposed for two different situations are based on the construction of a Poincaré map. The existence of certain kinds of homoclinic and heteroclinic connections between equilibria and/or periodic orbits is proved and their organization close to the T–point–Hopf bifurcation is described. The numerical phenomena found in Chua's equation strongly agree with the results deduced from the models.

Keywords: Global bifurcations; T-point; Hopf bifurcation; $\mathbb{Z}_2$-symmetry; Chua's equation.

1 Introduction

T–point heteroclinic cycles play an important role as organizing centers of the dynamics in the analysis of parameterized systems of autonomous ordinary differential equations (see, for example, [Glendinning and Sparrow, 1986; Bykov, 1993; Bykov, 1999; Bykov, 2000; Dumortier et al., 2000; Dumortier et al., 2001; Fernández–Sánchez et al., 2002; Krauskopf and Sieber, 2004; Dumortier et al., 2006] and references therein).

In three-dimensional systems having at least two saddle equilibria, a T–point occurs when the one-dimensional manifolds of those two equilibria coincide and, at the same time, the two–dimensional manifolds have a transversal intersection. In order to be precise, a T–point is a point of the space of parameters where such a heteroclinic cycle appears.

If the equilibria involved in the T–point heteroclinic cycle are saddle-foci then spiral curves of homoclinic connections of the two equilibria emerge from the T–point in the parameter plane [Bykov, 1999; Bykov, 2000]. Moreover, the T–point organizes a complex structure of bifurcations of periodic orbits. Thus, this is a rich bifurcation whose analysis is relevant in the understanding of three-

dimensional dynamics.

The work [Fernández–Sánchez et al., 2002] is devoted to the study of a T–point in a system with $\mathbb{Z}_2$-symmetry, that is, it is invariant to the change of variables $(x, y, z) \to (-x, -y, -z)$. In this case, the system has three equilibrium points (the origin and two nontrivial symmetric ones) and two symmetric T–point heteroclinic cycles coexist. This configuration leads to the appearance of three spiral curves of global bifurcations corresponding respectively to homoclinic connections to the origin, homoclinic connections to the nontrivial equilibria and heteroclinic connections between the nontrivial equilibria.

A T–point may exhibit degeneracies for several reasons (see, for instance, [Fernández–Sánchez et al., 2003; Fernández–Sánchez et al., 2004; Algaba et al., 2002; Algaba et al., 2003b; Homburg and Natiello, 2005]). One possibility is the interaction of a T–point heteroclinic cycle between two saddle-focus equilibria and a supercritical Hopf bifurcation of one of the equilibria. The study of the structures of global bifurcations close to this codimension–three bifurcation, called (supercritical) T–point–Hopf, is carried out in [Fernández–Sánchez et al., 2008]. The authors, by constructing a family of two-dimensional diffeomorphisms corresponding to the Poincaré map of a family of vector fields in $\mathbb{R}^3$ which exhibits a T–point–Hopf bifurcation, prove the existence and describe the location in the parameter space of homoclinic and heteroclinic connections between equilibria and/or periodic orbits, Shil'nikov-Hopf bifurcations, ... Moreover, taking into account the rich structure of homoclinic connection surfaces, a relationship between the T-point–Hopf bifurcation and the non-transverse Shil'nikov–Hopf bifurcation [Champneys and Rodríguez-Luis, 1999] is proved.

The first goal of this paper is to analyze the T–point–Hopf bifurcation in three-dimensional $\mathbb{Z}_2$-symmetric systems extending the ideas used in [Fernández–Sánchez et al., 2008]. Two different situations appear depending on the equilibrium (trivial or nontrivial) that exhibits the Hopf bifurcation. Thus, two models are constructed. The second aim of the work is to find and study numerically the

T–point–Hopf in Chua's equation.

The paper is organized as follows. In Sec. 2, we construct a family of diffeomorphisms, corresponding to the Poincaré map of a family of dynamical systems which exhibit a T–point–Hopf degeneration where the origin is the equilibrium that undergoes the (supercritical) Hopf bifurcation. Section 3 is devoted to the second case, namely, when the (subcritical) Hopf bifurcation is suffered by the nontrivial equilibria. In Sec. 4, the numerical analysis of the T–point–Hopf bifurcation in Chua's equation is performed. In this system, the Hopf bifurcation that originates the T–point–Hopf bifurcation corresponds to the nontrivial equilibria.

2 T–point–Hopf bifurcation of the origin

In the case of a supercritical Hopf bifurcation of the origin we are going to study a three-parametric family $\mathcal{X}_{d_1,d_2,\mu}$ of smooth (in variables and parameters) three-dimensional dynamical systems, for (d_1, d_2, μ) in a neighborhood of the origin, satisfying the following hypotheses:

(H1) *Every system of the family is invariant under the change of variables* $(x, y, z) \to (-x, -y, -z)$, *i.e., it is* $\mathbb{Z}_2$*-symmetric.*

(H2) *Every system of the family possesses three stationary points: one of them,* Q_1*, situated at the origin of the phase space and the other two,* Q_2^+ *and* Q_2^-*, which are mapped onto each other by the symmetry.*

(H3) *Near* Q_1 *it is possible to choose coordinates* (x, y, z) *in such a way that the flow, in a neighborhood of this equilibrium, is generated by the equations*

$$\begin{cases} \dot{r} &= r(\mu - r^2), \\ \dot{\nu} &= \omega, \\ \dot{z} &= \lambda z, \end{cases} \tag{1}$$

where (r, ν) are the polar coordinates of (x, y), ω does not vanish, λ is positive and μ is the principal parameter of the Hopf bifurcation.

Let us call Γ_1 the saddle periodic orbit that emerges, for $\mu > 0$, from the Hopf bifurcation of Q_1.

(H4) *Near Q_2^- it is possible to choose coordinates (X, Y, Z) in such a way that the flow, in a neighborhood of this equilibrium, is generated by the linear equations*

$$\begin{cases} \dot{X} &= PX - \Omega Y, \\ \dot{Y} &= \Omega X + PY, \\ \dot{Z} &= -\Lambda Z, \end{cases} \tag{2}$$

where P and Λ are positive numbers and Ω does not vanish.

Note that, using the $\mathbb{Z}_2$-symmetry, it is enough to work with one of the symmetrical equilibrium points (for example, Q_2^-) and the conclusions will be valid for the other one (Q_2^+).

In the neighborhoods of Q_1 and Q_2^- we can consider four transversal sections to the flow (see Figure 1) that can be defined, in the new coordinates, as

$$\begin{aligned} \Sigma_1 &= \{(x, y, z);\ z = h\}, \\ \Sigma_2 &= \{(X, Y, Z);\ Z = H\}, \\ \Sigma_3 &= \{(X, Y, Z);\ Y = 0\}, \\ \Sigma_4 &= \{(x, y, z);\ y = 0\}, \end{aligned} \tag{3}$$

where h and H are small enough positive numbers.

From now on, in this section, we take $\theta = -\omega/\lambda$, $\phi = (\omega/\lambda)\log h$, $\Delta = P/\Lambda$, $\Theta = \Omega/\Lambda$ and $\Phi = (-\Omega/\Lambda)\log H$.

(H5) *There exist two points $(X_0, 0, 0) \in \Sigma_3$, $(x_0, 0, 0) \in \Sigma_4$, with $X_0 > 0$ and $x_0 > 0$, and four numbers $A, B, C, D \in \mathbb{R}$, satisfying $C \neq 0$ and $AD - BC \neq 0$, such that the flow between Σ_3 and Σ_4,*

restricted to a neighborhood of $(X_0, 0, 0)$ *maps* $(X, 0, Z)$ *onto* $(x, 0, z)$ *where*

$$\begin{pmatrix} x - x_0 \\ \\ z \end{pmatrix} = \begin{pmatrix} A & B \\ \\ C & D \end{pmatrix} \begin{pmatrix} X - X_0 \\ \\ Z \end{pmatrix}. \tag{4}$$

(H6) *There exist four numbers* $a, b, c, d \in \mathbb{R}$*, satisfying* $ad - bc \neq 0$*, such that the flow between* Σ_1 *and* Σ_2*, restricted to a neighborhood of* $(0, 0, h)$*, maps* (x', y', h) *onto* (X', Y', H) *where*

$$\begin{pmatrix} X' \\ \\ Y' \end{pmatrix} = \begin{pmatrix} d_1 \\ \\ d_2 \end{pmatrix} + \begin{pmatrix} a & b \\ \\ c & d \end{pmatrix} \begin{pmatrix} x' \\ \\ y' \end{pmatrix}. \tag{5}$$

Let us explain these hypotheses. It is clear that hypotheses H1-H4 assure the existence of three equilibria: the symmetrical ones, $Q_2^{\pm}$, are saddle-focus and the origin, Q_1, undergoes a Hopf bifurcation.

With regard to equilibrium Q_1 we have decided to assume that the flow is generated, in a neighborhood of the equilibrium, by the normal form of a supercritical Hopf bifurcation truncated up to third order [Guckenheimer and Holmes, 1983; Kuznetsov, 2004]. Note that any three-dimensional system with a saddle-focus equilibrium having a non-degenerate supercritical Hopf bifurcation is locally topologically equivalent to system (1).

Concerning equilibrium Q_2^-, it is known [Hartman, 1960; Belitskii, 1973] that for any saddle-focus equilibrium there exists a local C^1 change of coordinates and time such that, in these coordinates, the flow is linear in a neighborhood of the equilibrium.

Once the coordinates have been chosen near the equilibria and the cross sections have been defined, it is necessary to give hypotheses to describe the flow between the equilibria.

The flow between Σ_3 and Σ_4 corresponds to the flow near the two-dimensional manifolds. In order to have a T–point heteroclinic cycle, both manifolds have to intersect transversally, which is assured

by the condition $C \neq 0$ of H5 (the intersection orbit will be called *closing orbit*). Note that the closing orbit has an infinitely many number of intersections with Σ_3 and Σ_4. To avoid this situation, it is necessary to restrict both sections. Thus we take in Σ_3 one small region around $(X_0, 0, 0)$, which is one of the infinitely many intersections of the closing orbit and Σ_3. In the same way, we choose in Σ_4 another small region around the point $(x_0, 0, 0)$, which is one of the infinitely many intersections of the closing orbit and Σ_4.

For the analysis of the global bifurcations performed in this section it is necessary that $x_0 > \sqrt{\mu}$ for $\mu > 0$. However, we do not have to add any new hypotheses because this condition is always valid for small values of μ, that is, close enough to the corresponding Hopf bifurcation.

Since the map generated by the flow between Σ_3 and Σ_4 is a diffeomorphism, it can be written as a Taylor expansion around $(X, Z) = (X_0, 0)$. In hypothesis H5 we have removed the higher-order terms to simplify the equations because they will not affect the low-order terms in the expressions we will obtain.

Analogous reasonings have been applied in hypothesis H6 to the map between Σ_1 and Σ_2 and its Taylor expansion around $(x, y) = (0, 0)$.

Schematic diagrams of the considered global connections in the phase space appear in Figs. 1–4. Fig. 5 shows, in the parameter space, the location of the heteroclinic cycles and the homoclinic orbits to Q_1 or Γ. From now on we will call EPC–point (Equilibrium-Periodic orbit Cycle) to a point of the space of parameter where a heteroclinic cycle between a periodic orbit and an equilibrium point appears. The main result of this section is the following theorem:

Theorem 2.1 (T–point–Hopf of the origin) *Consider a three-parametric family $\mathcal{X}_{d_1,d_2,\mu}$ of smooth (in variables and parameters) three-dimensional dynamical systems satisfying hypotheses H1-H6. Then, in a neighborhood of the origin of the space of parameters (d_1, d_2, μ), the following degeneracies exist:*

1. *A (supercritical) T–point–Hopf bifurcation for* $(d_1, d_2, \mu) = (0, 0, 0)$.

2. *A semi-straight line of T–points between* Q_1 *and* Q_2^- *given by* $(d_1, d_2) = (0, 0)$ *and* $\mu \leq 0$.

3. *An elliptical paraboloid of EPC–points between* Γ_1 *and* Q_2^-. *The paraboloid is given by*

$$\mu = \left\| \begin{pmatrix} a & b \\ c & d \end{pmatrix}^{-1} \begin{pmatrix} d_1 \\ d_2 \end{pmatrix} \right\|_2^2, \tag{6}$$

   where $\|\cdot\|_2$ *stands for the euclidean norm.*

4. *One cylindrical surface, with logarithmic spiral cross section, of homoclinic connections to* Q_1.

   The equations of this surface, parameterized by Z *and* $\mu < 0$, *are*

$$\begin{pmatrix} d_1 \\ d_2 \end{pmatrix} = \left(X_0 - \frac{D}{C} Z \right) Z^{\Delta} H^{-\Delta} \begin{pmatrix} \cos(\Theta \log Z + \Phi) \\ \sin(\Theta \log Z + \Phi) \end{pmatrix}.$$

5. *A logarithmic spiral of Shil'nikov-Hopf bifurcations whose equations, parameterized by* Z, *are*

$$\begin{pmatrix} d_1 \\ d_2 \end{pmatrix} = \left(X_0 - \frac{D}{C} Z \right) Z^{\Delta} H^{-\Delta} \begin{pmatrix} \cos(\Theta \log Z + \Phi) \\ \sin(\Theta \log Z + \Phi) \end{pmatrix},$$

   when $\mu = 0$.

6. *A solid region of homoclinic connections to* Γ_1 *whose equations, parameterized by* $s \in [0, 2\pi)$, $Z > 0$ *and* $\mu > 0$, *are*

$$\begin{pmatrix} d_1 \\ d_2 \end{pmatrix} = -\begin{pmatrix} a & b \\ c & d \end{pmatrix} \begin{pmatrix} \sqrt{\mu}\cos(s) \\ \sqrt{\mu}\sin(s) \end{pmatrix} + \left(X_0 - \frac{D}{C} Z \right) Z^{\Delta} H^{-\Delta} \begin{pmatrix} \cos(\Theta \log Z + \Phi) \\ \sin(\Theta \log Z + \Phi) \end{pmatrix}.$$

   For every point of this region there are also heteroclinic connections between Q_1 *and* Γ_1.

7. *A surface of homoclinic connections to* Q_2^- *whose equations are*

$$\begin{pmatrix} d_1 \\ d_2 \end{pmatrix} = -\hat{r} \left(\tau\left(\Sigma_4, \Sigma_1\right); x_0 + \frac{A}{C} z, \mu \right) \begin{pmatrix} a & b \\ c & d \end{pmatrix} \begin{pmatrix} \cos(\theta \log z + \phi) \\ \sin(\theta \log z + \phi) \end{pmatrix},$$

where

$$\hat{r}(\tau(\Sigma_4,\Sigma_1);x,\mu)=\begin{cases} xz^{-\frac{\mu}{\lambda}}h^{\frac{\mu}{\lambda}}\sqrt{\dfrac{\mu}{\mu-x^2+x^2z^{-\frac{2\mu}{\lambda}}h^{\frac{2\mu}{\lambda}}}} & \text{if} \quad \mu\neq 0, \\ \dfrac{x}{\sqrt{1+\dfrac{2x^2}{\lambda}\log\left(\dfrac{h}{z}\right)}} & \text{if} \quad \mu=0. \end{cases} \tag{7}$$

8. *A surface of heteroclinic connections between Q_2^- and Q_2^+ whose equations are*

$$\begin{pmatrix} d_1 \\ \\ d_2 \end{pmatrix}=\hat{r}\left(\tau\left(\Sigma_4,\Sigma_1\right);x_0-\frac{A}{C}z,\mu\right)\begin{pmatrix} a & b \\ \\ c & d \end{pmatrix}\begin{pmatrix} \cos(\theta\log z+\phi) \\ \\ \sin(\theta\log z+\phi) \end{pmatrix},$$

where $\hat{r}$ is given by (7).

Note that, due to the $\mathbb{Z}_2$-symmetry, each global connection considered in the theorem has a symmetric one for the same value of the parameters. Moreover, the surfaces given in items 7 and 8 are symmetric, up to first order, with respect to $(d_1,d_2)=(0,0)$.

PROOF:

The existence of the global connections described in Theorem 2.1 (items 1-7) can be proved without considering the $\mathbb{Z}_2$-symmetry. So, the results obtained in [Fernández–Sánchez et al., 2008] can be applied. Nevertheless, for the sake of completeness, we give an outline of the proof.

Let us begin by considering the case $\mu\leq 0$.

From H6, the one-dimensional unstable manifold of Q_1, which corresponds to $(x',y')=(0,0)$ in Σ_1, intersects Σ_2 with coordinates $(X',Y')=(d_1,d_2)$.

The one-dimensional stable manifold of Q_2^- has coordinates $(X',Y')=(0,0)$ in Σ_2; therefore, if $(d_1,d_2)=(0,0)$ then there exists a heteroclinic orbit between Q_1 and Q_2^-. Moreover, since $C\neq 0$, the two-dimensional manifolds of Q_1 and Q_2^- have a transversal intersection, which corresponds to the closing orbit. Joining both orbits a T–point heteroclinic cycle is obtained.

Items 1 and 2 are a direct conclusion from this result.

If the one-dimensional unstable manifold of Q_1 intersects the two-dimensional stable manifold of Q_1 then a homoclinic orbit appears. Let us follow such a homoclinic orbit.

On the one hand, we have seen that the coordinates of the one-dimensional unstable manifold of Q_1 in Σ_2 are (d_1, d_2, H). On the other hand, a orbit belongs to the two-dimensional manifold of Q_1 if it intersects Σ_4 with z-coordinate equal to 0. That is, there exist a point $(X, 0, Z) \in \Sigma_3$ such that, by H5,

$$\begin{pmatrix} x - x_0 \\ \\ 0 \end{pmatrix} = \begin{pmatrix} A & B \\ \\ C & D \end{pmatrix} \begin{pmatrix} X - X_0 \\ \\ Z \end{pmatrix},$$

which implies that $X = X_0 - \frac{D}{C}Z$. The flow given by system (2) has to map $(d_1, d_2, H) \in \Sigma_2$ to $(X_0 - \frac{D}{C}Z, 0, Z) \in \Sigma_3$. By integrating system (2) and using this condition, items 4 and 5 are obtained.

Let us consider now the case $\mu > 0$. The intersection between the unstable manifold of the periodic orbit Γ_1 and Σ_1 is a circle (see Fig. 6) that can be parameterized by $(x', y') = \sqrt{\mu}(\cos(s), \sin(s))$ for $s \in [0, 2\pi)$. The same ideas used for $(x', y') = (0, 0)$ in the case $\mu \leq 0$ can be now applied to the points of the circle to obtain items 3 and 6.

Concerning item 7, a homoclinic connection of Q_2^- intersects Σ_3 in a point $(X, 0, 0)$. Mapping this point by using the expression of the flow given in H5, we obtain the point $(x_0 + \frac{A}{C}z, 0, z) \in \Sigma_4$. The orbit obtained from the integration of non-linear system (1) with initial condition $(r(0), \nu(0), z(0)) = (x_0 + \frac{A}{C}z, 0, z)$, intersects Σ_1 with coordinates

$$\begin{pmatrix} x' \\ \\ y' \end{pmatrix} = \hat{r}\left(\tau\left(\Sigma_4, \Sigma_1\right); x_0 + \frac{A}{C}z, \mu\right) \begin{pmatrix} \cos(\theta \log z + \phi) \\ \\ \sin(\theta \log z + \phi) \end{pmatrix},$$

where $\hat{r}$ is given by Eq. (7).

Taking into account that the orbit must be the one dimensional manifold of Q_2^-, that is, $(X', Y') = (0, 0)$, and applying the expression of the flow given in H6 item 7 is proved.

Item 8 is directly provided by the $\mathbb{Z}_2$-symmetry. So, these heteroclinic connections do not appear in [Fernández–Sánchez et al., 2008]. Let us prove this item.

The heteroclinic connections between Q_2^- and Q_2^+ can be studied in the following way. Such a curve has to intersect section Σ_3, in a neighborhood of $(X_0, 0, 0)$, with coordinates $(X, 0, 0)$, because $Z = 0$ is the equation of the two-dimensional unstable manifold of Q_2^-.

The flow maps this point to $(x, 0, -z) \in \Sigma_4$, whose coordinates are

$$\begin{pmatrix} x \\ \\ -z \end{pmatrix} = \begin{pmatrix} x_0 \\ \\ 0 \end{pmatrix} + \begin{pmatrix} A & B \\ \\ C & D \end{pmatrix} \begin{pmatrix} X - X_0 \\ \\ 0 \end{pmatrix}. \tag{8}$$

The first coordinate of this point is positive, because it belongs to a neighborhood of $(x_0, 0, 0)$. However, the third coordinate is negative because, in other case, the point would be reinjected by the flow to Q_2^-.

From system (8) it is possible to obtain $x = x_0 - \frac{A}{C}z$. The orbit corresponding to the point $(x_0 - \frac{A}{C}z, 0, -z)$ reaches Q_2^+ following its one-dimensional stable manifold. Due to the symmetry, the orbit corresponding to the point $(-x_0 + \frac{A}{C}z, 0, z)$ has to reach Q_2^- following its one-dimensional stable manifold.

Let us consider system (1) with the initial condition $(r(0), \nu(0), z(0))=(x_0 - \frac{A}{C}z, \pi, z)$, i.e. the point $(-x_0 + \frac{A}{C}z, 0, z)$. The solution is

$$\begin{pmatrix} x(t) \\ \\ y(t) \\ \\ z(t) \end{pmatrix} = \begin{pmatrix} \hat{r}(t; x_0 - \frac{A}{C}z, \mu)\cos(\omega t + \pi) \\ \\ \hat{r}(t; x_0 - \frac{A}{C}z, \mu)\sin(\omega t + \pi) \\ \\ ze^{\lambda t} \end{pmatrix} = \begin{pmatrix} -\hat{r}(t; x_0 - \frac{A}{C}z, \mu)\cos(\omega t) \\ \\ -\hat{r}(t; x_0 - \frac{A}{C}z, \mu)\sin(\omega t) \\ \\ ze^{\lambda t} \end{pmatrix}, \tag{9}$$

where $\hat{r}$ is the solution of the radial equation of (1) with $\hat{r}(0) = r_0$ which is given by

$$\hat{r}(t; r_0, \mu) = \begin{cases} r_0 e^{\mu t}\sqrt{\dfrac{\mu}{\mu - r_0^2 + r_0^2 e^{2\mu t}}} & \text{if} \quad \mu \neq 0, \\ \\ \dfrac{r_0}{\sqrt{1 + 2t r_0^2}} & \text{if} \quad \mu = 0. \end{cases} \tag{10}$$

The flight time this orbit needs to go from the point $(-x_0 + \frac{A}{C}z, 0, z)$ to Σ_1 is

$$\tau(\Sigma_4, \Sigma_1) = \frac{1}{\lambda}\log\left(\frac{h}{z}\right).$$

Substituting this time into Eq. (9) we get the point $(x', y', h) \in \Sigma_1$, where

$$\begin{pmatrix} x' \\ \\ y' \end{pmatrix} = \hat{r}\left(\tau(\Sigma_4, \Sigma_1); x_0 - \frac{A}{C}z, \mu\right) \begin{pmatrix} \cos(\theta \log z + \phi) \\ \\ \sin(\theta \log z + \phi) \end{pmatrix}.$$

Finally, the flow maps the point $(x', y', h) \in \Sigma_1$ to the point $(0, 0, H) \in \Sigma_2$ because it belongs to the one-dimensional stable manifold of Q_2^-. Using the map given in Eq. (5) and solving the equations for d_1 and d_2, the following equations are obtained

$$\begin{pmatrix} d_1 \\ \\ d_2 \end{pmatrix} = R\left(\tau\left(\Sigma_4, \Sigma_1\right); x_0 - \frac{A}{C}z, \mu\right) \begin{pmatrix} a & b \\ \\ c & d \end{pmatrix} \begin{pmatrix} \cos(\theta \log z + \phi) \\ \\ \sin(\theta \log z + \phi) \end{pmatrix}. \tag{11}$$

3 T–point–Hopf bifurcation of the non-trivial equilibria

In the case of a subcritical Hopf bifurcation of the non-trivial equilibria, we are going to consider a three-parametric family $\mathcal{X}_{d_1,d_2,M}$ of smooth (in variables and parameters) three-dimensional dynamical systems, for (d_1, d_2, M) in a neighborhood of the origin, satisfying hypotheses H1, H2, H5, H6 and these two new ones:

(H7) *Near Q_1 it is possible to choose coordinates (x, y, z) in such a way that the flow, in a neighborhood of this equilibrium, is generated by the linear equations*

$$\begin{cases} \dot{x} &= -px - \omega y, \\ \\ \dot{y} &= \omega x - py, \\ \\ \dot{z} &= \lambda z, \end{cases} \tag{12}$$

where p and λ are positive numbers and ω does not vanish.

(H8) *Near Q_2^- it is possible to choose coordinates (X, Y, Z) in such a way that the flow, in a neighborhood of this equilibrium, is generated by the equations*

$$\begin{cases} \dot{R} &= -R(M - R^2), \\ \dot{N} &= \Omega, \\ \dot{Z} &= -\Lambda Z, \end{cases} \tag{13}$$

where (R, N) are the polar coordinates of (X, Y), Ω does not vanish, Λ is positive and M is the principal parameter of the Hopf bifurcation.

Let us call $\Gamma_2^{\pm}$ the saddle periodic orbits that emerge, for $M > 0$, from the Hopf bifurcation of $Q_2^{\pm}$, respectively.

From now on, in this section, we take $\Theta = \Omega/\Lambda$, $\Phi = -(\Omega/\Lambda)\log H$, $\delta = p/\lambda$, $\theta = -\omega/\lambda$ and $\phi = (\omega/\lambda)\log h$.

For the analysis of the global bifurcations performed in this section it is necessary that $X_0 > \sqrt{M}$ for $M > 0$. However, we do not have to add any new hypotheses because this condition is always valid for small values of M, that is, close enough to the corresponding Hopf bifurcation.

Theorem 3.1 (T–point–Hopf of the non-trivial equilibria) *Consider a three-parametric family $\mathcal{X}_{d_1,d_2,M}$ of smooth (in variables and parameters) three-dimensional dynamical systems satisfying hypotheses H1, H2 and H5-H8. Then, in a neighborhood of the origin of the space of parameters (d_1, d_2, M), the following degeneracies exist:*

1. *A (subcritical) T–point–Hopf bifurcation for $(d_1, d_2, M) = (0, 0, 0)$.*

2. *A semi-straight line of T–points between Q_1 and Q_2^- given by $(d_1, d_2) = (0, 0)$ and $M \leq 0$.*

3. *A paraboloid of EPC–points between Γ_2^- and Q_1 given by $M = d_1^2 + d_2^2$.*

4. *One cylindrical surface of homoclinic connections to Q_2^-. The equations of this surface, parameterized by z and $M < 0$, are*

$$\begin{pmatrix} d_1 \\ \\ d_2 \end{pmatrix} = -\left(x_0 + \frac{A}{C}z\right) z^{\delta} h^{-\delta} \begin{pmatrix} \cos(\theta \log z + \phi) \\ \\ \sin(\theta \log z + \phi) \end{pmatrix}.$$

5. *One cylindrical surface of heteroclinic connections between Q_2^- and Q_2^+ whose equations, parameterized by z and $M < 0$, are*

$$\begin{pmatrix} d_1 \\ \\ d_2 \end{pmatrix} = \left(x_0 - \frac{A}{C}z\right) z^{\delta} h^{-\delta} \begin{pmatrix} \cos(\theta \log z + \phi) \\ \\ \sin(\theta \log z + \phi) \end{pmatrix}.$$

This surface is symmetric, up to first order, to the surface of the previous item respect to $(d_1, d_2) = (0, 0)$.

6. *A logarithmic spiral of homoclinic Shil'nikov-Hopf bifurcations of Q_2^- whose equations, parameterized by z, are*

$$\begin{pmatrix} d_1 \\ \\ d_2 \end{pmatrix} = -\left(x_0 + \frac{A}{C}z\right) z^{\delta} h^{-\delta} \begin{pmatrix} \cos(\theta \log z + \phi) \\ \\ \sin(\theta \log z + \phi) \end{pmatrix}$$

when $M = 0$.

7. *A logarithmic spiral of heteroclinic Shil'nikov-Hopf bifurcations between Q_2^- and Q_2^+ whose equations, parameterized by z are*

$$\begin{pmatrix} d_1 \\ \\ d_2 \end{pmatrix} = \left(x_0 - \frac{A}{C}z\right) z^{\delta} h^{-\delta} \begin{pmatrix} \cos(\theta \log z + \phi) \\ \\ \sin(\theta \log z + \phi) \end{pmatrix}$$

when $M = 0$. This curve is symmetric, up to first order, to the curve of the previous item respect to $(d_1, d_2) = (0, 0)$.

8. *A solid region of homoclinic connections to Γ_2^- whose equations, parameterized by $s \in [0, 2\pi)$, $z > 0$ and $M > 0$, are*

$$\begin{pmatrix} d_1 \\ \\ d_2 \end{pmatrix} = \begin{pmatrix} \sqrt{M}\cos(s) \\ \\ \sqrt{M}\sin(s) \end{pmatrix} - \left(x_0 + \frac{A}{C}z\right) z^{\delta} h^{-\delta} \begin{pmatrix} a & b \\ \\ c & d \end{pmatrix} \begin{pmatrix} \cos(\theta \log z + \phi) \\ \\ \sin(\theta \log z + \phi) \end{pmatrix}.$$

For every point of this region there are also heteroclinic connections between Q_2^- and Γ_2^-.

9. *A solid region of heteroclinic connections between* Γ_2^- *and* Γ_2^+ *whose equations, parameterized by* $s \in [0, 2\pi)$, $z > 0$ *and* $M > 0$, *are*

$$\begin{pmatrix} d_1 \\ d_2 \end{pmatrix} = \begin{pmatrix} \sqrt{M}\cos(s) \\ \sqrt{M}\sin(s) \end{pmatrix} + \left(x_0 - \frac{A}{C}z\right) z^{\delta} h^{-\delta} \begin{pmatrix} a & b \\ c & d \end{pmatrix} \begin{pmatrix} \cos(\theta \log z + \phi) \\ \sin(\theta \log z + \phi) \end{pmatrix}.$$

This region is symmetric, up to first order, to the region of the previous item respect to $(d_1, d_2) = (0, 0)$. *For every point of this region there are also heteroclinic connections between* Q_2^- *and* Γ_2^+.

10. *A surface of homoclinic connections to* Q_1 *whose equations are*

$$\begin{pmatrix} d_1 \\ d_2 \end{pmatrix} = \hat{R}\left(\tau\left(\Sigma_3, \Sigma_2\right); X_0 - \frac{D}{C}Z, M\right) \begin{pmatrix} \cos(\Theta \log Z + \Phi) \\ \sin(\Theta \log Z + \Phi) \end{pmatrix},$$

where

$$\hat{R}(\tau(\Sigma_3, \Sigma_2); X, M) = \begin{cases} XZ^{-\frac{M}{\Lambda}} H^{\frac{M}{\Lambda}} \sqrt{\dfrac{M}{M - X^2 + X^2 Z^{-\frac{2M}{\Lambda}} H^{\frac{2M}{\Lambda}}}} & \text{if} \quad M \neq 0, \\ \dfrac{X}{\sqrt{1 + \dfrac{2X^2}{\Lambda} \log\left(\dfrac{H}{Z}\right)}} & \text{if} \quad M = 0. \end{cases} \tag{14}$$

Note that, due to the $\mathbb{Z}_2$-symmetry, each global connection considered in the theorem has a symmetric one for the same value of the parameters. The equations of the bifurcation sets considered in Theorem 3.1 can be derived as those in Theorem 2.1. So, the proof of Theorem 3.1 is omitted.

4 Application to Chua's Equation

Chua's equation models a simple electronic circuit exhibiting a wide range of complex dynamical behaviours. Such equation is derived in [Pivka et al., 1996] considering the case of a cubic nonlinearity:

$$\begin{aligned} \dot{x} &= \alpha(y - ax^3 - cx), \\ \dot{y} &= x - y + z, \\ \dot{z} &= -\beta y - \gamma z. \end{aligned} \tag{15}$$

A parameter γ is included in this equation in order to take into account small resistive effects in the inductance of the circuit.

In this numerical study of Chua's equation (15), done using AUTO [Doedel et al., 1998], β, c and α are taken as bifurcation parameters and the other two are fixed, namely $a = -1$, $\gamma = 0.3 > 0$, in accordance with previous works (see [Algaba et al., 2002; Algaba et al., 2003a; Algaba et al., 2003b; Algaba et al., 2006]).

In Fig. 7(a), the projection of the T-points curve, **TP**, onto the (α, β) plane is shown. It has been obtained by numerical continuation in the three-parameter space (α, β, c). As can be noticed, it emerges from a triple-zero linear degeneracy point of the origin **TZ**, that exists for $\alpha = -1.373125$, $\beta = 0.016875$ and $c \approx 0.946746$ (see [Algaba et al., 2003a] for details; concretely, this curve appears in Fig.12). The end of the curve occurs when it meets the (subcritical) Hopf surface of the nontrivial equilibria **h**, giving rise to a T-point Hopf, **TPH**, whose coordinates are $(\alpha, \beta, c) \approx (-1.654942, 0.048508, 0.957893)$. Moreover, the **TP** curve has a fold, it exhibits a transversality failure with respect to α (a maximum occurs for $\alpha_c \approx -1.34156$, see [Algaba et al., 2003b]).

In Fig. 7(b) the projection onto the xz-plane of one of such T-points is shown. It is the easiest one that connects the origin and one of the nontrivial equilibria (observe the one-dimensional manifold, black line, joining both equilibria), for that reason it will be called principal T-point.

According to the above theoretical analysis, the curves of Hopf-Shil'nikov degeneracies emerge spiraling from the T-point Hopf **TPH** (see their projections onto the (α, β) plane in Fig. 8). One of these curves **SHn** corresponds to the homoclinic connections to the nontrivial equilibria whereas the curve **SHe2** is of heteroclinic connections between nontrivial equilibria. As can be observed, these two curves spiral in opposite senses. Moreover, a bi-spiraling phenomenom appears in both cases [Fernández–Sánchez et al., 2003; Fernández–Sánchez et al., 2004]: the curve starts from **TPH**, and later it re-enters at the same point.

A third curve of Hopf-Shil'nikov degeneracies exists on the Hopf surface of the nontrivial equilibria **h**. For the sake of clarity, it has not been drawn in Fig. 8 since it is not related to the point **TPH**. This curve, that will be called in the following **SHe**, corresponds to a degeneracy exhibited by the curve of heteroclinic connections of the nontrivial equilibria **He**, curve that connects a Takens-Bogdanov point and the T-Point **TP** (as it will be seen in Fig. 9 (a)).

In order to understand the evolution of the form of global connections loci in the three-parameter space in the vicinity of the point **TPH**, bi-dimensional slices in the (β, c) plane will be taken, for several different values of parameter α: from $\alpha = -1.41$ till $\alpha = -1.9$ (observe this range in Fig. 8(a)). In these figures, we will mark the Shil'nikov-Hopf points in the following manner: blue filled circles for the points of curve **SHe2**, red filled circles for the points of curve **SHn**, and brown filled squares for the points of **SHe**.

The first bifurcation set considered corresponds to $\alpha = -1.41$ (see Fig. 9). Three codimension-two points appear: a Takens-Bogdanov bifurcation of the origin, **TB**, a principal T-point **TP** and a secondary T-point **TP2**. A curve of heteroclinic connections **He** joins the points **TB** and **TP**. Note that **He** is close to have an intersection with the curve of Hopf of the nontrivial equilibria **h**. From the point **TP** (see [Fernández–Sánchez et al., 2002]) a curve of homoclinic connections of the origin **Hom** and a curve of homoclinic connections of the nontrivial equilibria **Hn** also emerge. Note that **Hn** exhibits a bi-spiraling behavior. Moreover, a curve of heteroclinic bifurcations of the nontrivial equilibria **He2** connects the points **TP** and **TP2** (although this curve passes close to the point **TB**, it is not related to it). Since the T-point Hopf **TPH** exhibited by Chua's equation corresponds to a Hopf of the nontrivial equilibria **h**, the curve **Hom** will not be shown in the following bifurcation sets.

In Fig. 9(b) the projection onto the xz-plane of the secondary T-point **TP2** is shown. Observe that its one-dimensional manifold (black line) joining both equilibria is *more complicated* than the one-dimensional manifold of the principal T-point **TP**.

In Fig. 10 projections onto the xz plane of the global connections that appear in Fig. 9(a), **Hom**, **Hn**, **He** and **He2** are drawn. Note that the difference between the shapes of the heteroclinic connections **He** and **He2** is a direct consequence of the different T–points they are related to (see Figs. 7(b) and 9(b)).

Decreasing α a first non-transverse contact between the curves **He** and **h** appears for $\alpha \approx -1.417965$: it is a non-transverse Shil'nikov-Hopf bifurcation (of the forward-pointing case) [Champneys and Rodríguez-Luis, 1999]. Then, for $\alpha = -1.45$ two Hopf-Shil'nikov points **SHe** exist (see Fig. 11). Now, it can be clearly observed that the curve **He**2 is not related to the point **TB**.

For the next α-slice depicted in Fig. 12, $\alpha = -1.64$, eight new Hopf-Shil'nikov points appear, since four non-transverse Shil'nikov-Hopf points has occurred, two of curve **He**2 (for $\alpha \approx -1.63378$ and $\alpha \approx -1.604095$), one of **He** (for $\alpha \approx -1.5$) and another one of **Hn** (for $\alpha \approx -1.4667$). The most outer correspond to the curve **SHe** (as stated above, this curve is not related to the point **TPH**), whereas the other six belong, two to the curve **SHn** and four to **SHe**2. Note that the new two points **SHe** are originated by the intersection between the curves **He**2 and **h**. Analogously, the new four points **SHe**2 correspond to intersections of the two heteroclinic curves **He** and **He**2 with the Hopf curve **h**.

In the new slice, for $\alpha = -1.645$ (see Fig. 13) the point **TP** continues approaching more and more to Hopf's surface **h**. In this case four new points appear **SHn** as a consequence of two non-transversal Shil'nikov-Hopf of curve **Hn** ($\alpha \approx -1.64178$, and $\alpha \approx -1.64313$). Note that the curves of homoclinic and heteroclinic connections to the nontrivial equilibria are arranged in pairs due to the bi-spiraling phenomenon.

When parameter α crosses the critical value where the point **TPH** occurs (at this moment infinitely many points of both curves **SHn** and **SHe**2 exist), we are going to see a sequence of fitted curves: the curves **He**2 and **He** of heteroclinic connections alternate with the curves of **Hn** (see Fig. 14). The remainders of the curves of global connections are going to be eliminated in non-transverse Shil'nikov-

Hopf points (of downward-pointing case) [Champneys and Rodríguez-Luis, 1999].

For the following value of α considered on the other side of **TPH**, $\alpha = -1.7$ (see Fig. 15 (a)), even nine Shil'nikov-Hopf points stay, four correspond to the homoclinic connection **Hn** and the rest to heteroclinic orbits.

The first points that disappear, for $\alpha \approx -1.72121$ and $\alpha \approx -1.73547$, are those of the curve **SHn**. Thus, the curve **Hn** already does not exist when $\alpha = -1.79$ (see Fig. 15 (b)). Regarding the remainders of the curves of heteroclinic connections, they have a contact, before their disappearance in non-transverse Shil'nikov-Hopf points (of downward pointing case). Such a contact is necessary in order that they could disappear, since, as can be seen in Fig. 15(b), they are joining two Shil'nikov-Hopf points of different curves, **SHe** and **SHe**2.

After that contact, as can be observed in Fig. 15(c), for $\alpha = -1.795$, the remainders of the heteroclinic curves are joining Hopf-Shil'nikov points of the same curve. In this manner, the pieces of such curves may disappear.

In Fig. 15(d), for $\alpha = -1.9$, curve **He** has already disappeared, for $\alpha \approx -1.81044$, and curve **He**2 disappears for $\alpha \approx -1.93608$. On the other hand, the curve **He** continues joining the points **TB** and **SHe**. The previous slices of the parameter space show how complicated the surface of heteroclinic connections of the nontrivial equilibria is: although curves **He** and **He**2 seemed to be independent in the first slices, actually they belong to the same surface.

To finish this numerical study, a homoclinic connection to the origin **Hom** is shown in Fig. 16. The temporal wave $x(t)$ confirms that these homoclinic connections are good approximations to the cycles between periodic orbit and equilibrium: in the first part of the pulse it approximates the connection between the equilibrium and the periodic orbit and in the second one it is close to the connection between the periodic orbit and the equilibrium.

Acknowledgements

This work has been partially supported by the *Ministerio de Educación y Ciencia, Plan Nacional I+D+I* co-financed with FEDER funds, in the frame of the project MTM2007-64193 and by the *Consejería de Educación y Ciencia de la Junta de Andalucía* (FQM-276, TIC-0130 and P08-FQM-03770).

References

Algaba, A., F. Fernández–Sánchez, E. Freire, M. Merino, and A. J. Rodríguez-Luis [2002]. Non-transversal curves of T-points: a source of closed curves of global bifurcations. *Physics Letters* **A303**, 204–211.

Algaba, A., M. Merino, E. Freire, E. Gamero, and A. J. Rodríguez-Luis [2003a]. Some results on Chua's equation near a triple-zero linear degeneracy. *International Journal of Bifurcation and Chaos*, **13**, 583-608.

Algaba, A., M. Merino, F. Fernández–Sánchez and A. J. Rodríguez-Luis [2003b]. Closed curves of global bifurcations in Chua's equation: a mechanism for their formation. *International Journal of Bifurcation and Chaos*, **13**, 609–616.

Algaba, A., M. Merino, F. Fernández–Sánchez and A. J. Rodríguez-Luis [2006]. Open-to-closed curves of saddle-node bifurcations of periodic orbits near a nontransversal T-point in Chua's equation. *International Journal of Bifurcation and Chaos*, **16**, 2637–2647.

Belitskii, G. R. [1973]. Functional equations and conjugacy of local diffeomorphisms of a finite smoothness class. *Functional Anal. Appl.* **7**, 268–277.

Bykov, V. V. [1993]. The bifurcations of separatrix contours and chaos. *Physica D* **62**, 290–299.

Bykov, V. V. [1999]. On systems with separatrix contour containing two saddle-foci. *Journal of Mathematical Sciences* **95**, 2513–2522.

Bykov, V. V. [2000]. Orbits structure in a neighborhood of a separatrix cycle containing two saddle-foci.*American Mathematical Society Translations, Series 2* **200**, 87–97.

Champneys, A. R. and A. J. Rodríguez-Luis [1999]. The non-transverse Shil'nikov-Hopf bifurcation; uncoupling of homoclinic orbits and homoclinic tangencies, *Physica D* **128**, 130–158.

Doedel, E. J., A. R. Champneys, T. F. Fairgrieve, Y. A. Kuznetsov, B. Sandstede, and X. Wang [1998]. AUTO97: continuation and bifurcation software for ordinary differential equations (with HomCont).

Dumortier, F. and Kokubu, H. [2000]. Chaotic dynamics in $\mathbb{Z}_2$-equivariant unfoldings of codimension three singularities of vector fields in $\mathbb{R}^3$, *Ergod. Th. & Dynam. Sys.* **20**, 85–107.

Dumortier, F., Ibáñez, S. and Kokubu, H. [2001]. New aspects in the unfolding of the nilpotent singularity of codimension three, *Dynamical Systems* **16**, 63–95.

Dumortier, F., Ibañez, S. and Kokubu, H. [2006]. Cocoon bifurcation in three-dimensional reversible vector fields *Nonlinearity* **19**, 305–328.

Fernández–Sánchez, F., E. Freire, and A. J. Rodríguez–Luis [2002]. T-points in a $\mathbb{Z}_2$-symmetric electronic oscillator. (I) Analysis. *Nonlinear Dynamics* **28**, 53–69.

Fernández–Sánchez, F., E. Freire, L. Pizarro and A.J. Rodríguez–Luis [2003]. A model for the analysis of the dynamical consequences of a nontransversal intersections of the two-dimensional manifolds involved in a T–point. *Phys. Lett. A* **320**,169–179.

Fernández–Sánchez, F., E. Freire and A.J. Rodríguez–Luis [2004]. Bi-spiraling homoclinic curves around a T–point in Chua's equation. *Int. J. Bifurcation and Chaos* **14**, 1789–1793.

Fernández–Sánchez, F., E. Freire, and A. J. Rodríguez–Luis [2008]. Analysis of the T-point-Hopf bifurcation. *Physica D* **237**, 292–305.

Glendinning, P. and C. Sparrow [1986]. Bifurcations near homoclinic orbits with symmetry. *Journal of Statistical Physics* **43**, 479–488.

Guckenheimer, J. and P. J. Holmes [1983]. *Nonlinear Oscillations, Dynamical Systems, and Bifurcations of Vector Fields* (Springer-Verlag, NY).

Hartman, P. [1960]. On Local Homomorphisms of Euclidean Spaces. *Bol. Soc. Math. Mexicana* **5**, 220–241.

Homburg, A. and M. A. Natiello [2005]. Accumulations of T-points in a model for solitary pulses in an excitable reaction-diffusion medium, *Physica D* **201**, 212–229.

Krauskopf, B. and Sieber, J. [2004]. Bifurcation analysis of an inverted pendulum with delayed feedback control near a triple-zero eigenvalue singularity, *Nonlinearity* **17**, 85–103.

Kuznetsov, Yu. [2004]. *Elements of Applied Bifurcation Theory* (Springer-Verlag, NY).

Pivka, L., C. W. Wu, and A. Huang [1996]. Lorenz equation and Chua's equation. *International Journal of Bifurcation and Chaos* **6**, 2443–2489.

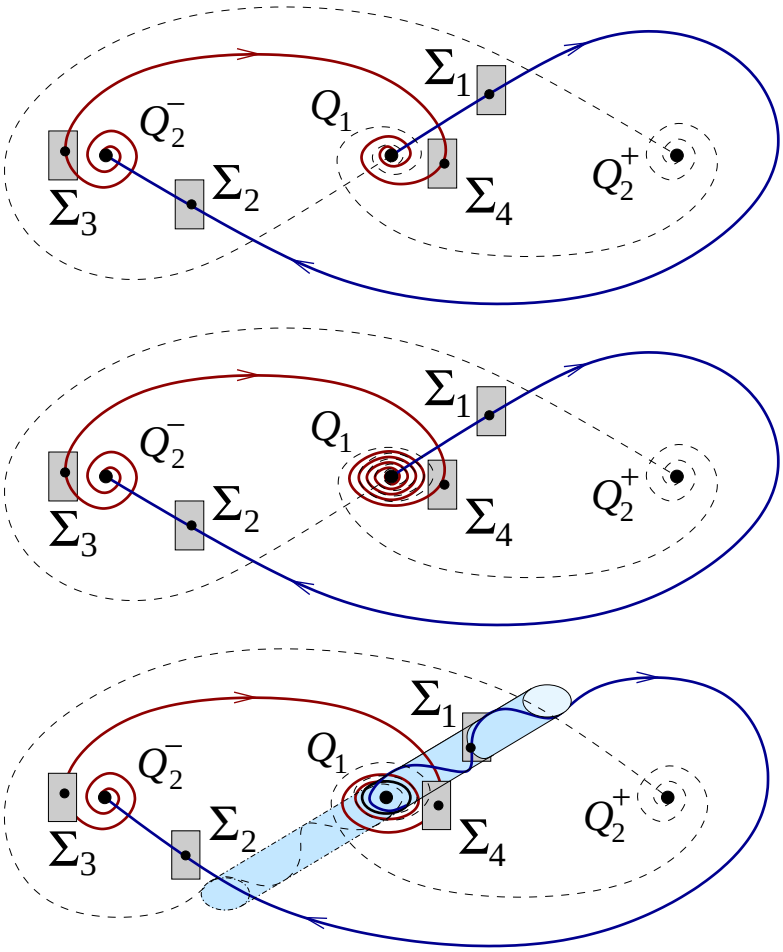

Figure 1: Different types of heteroclinic cycles depending on the values of μ. The transversal sections used in the construction of the full Poincaré map and the two-dimensional unstable manifold of Γ (for $\mu > 0$) have been also sketched.

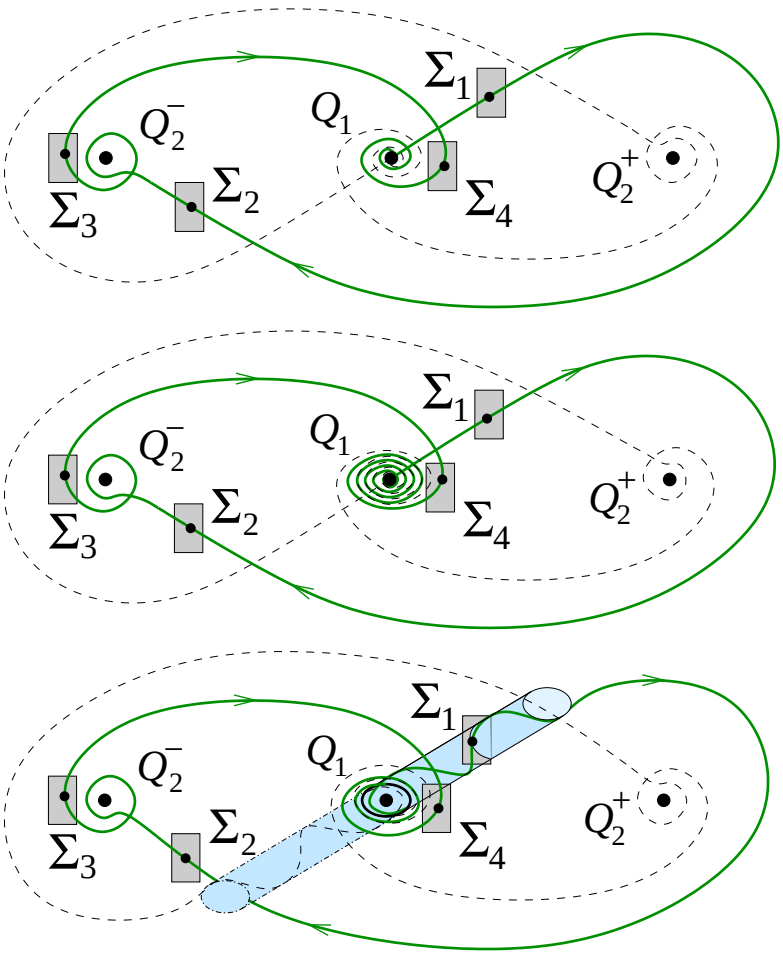

Figure 2: Schematic diagram of homoclinic connections to Q_1 and Γ depending on the value of μ. We have also drawn the transversal sections needed in the construction of the Poincaré map and the unstable cylinder of the periodic orbit Γ (for $\mu > 0$).

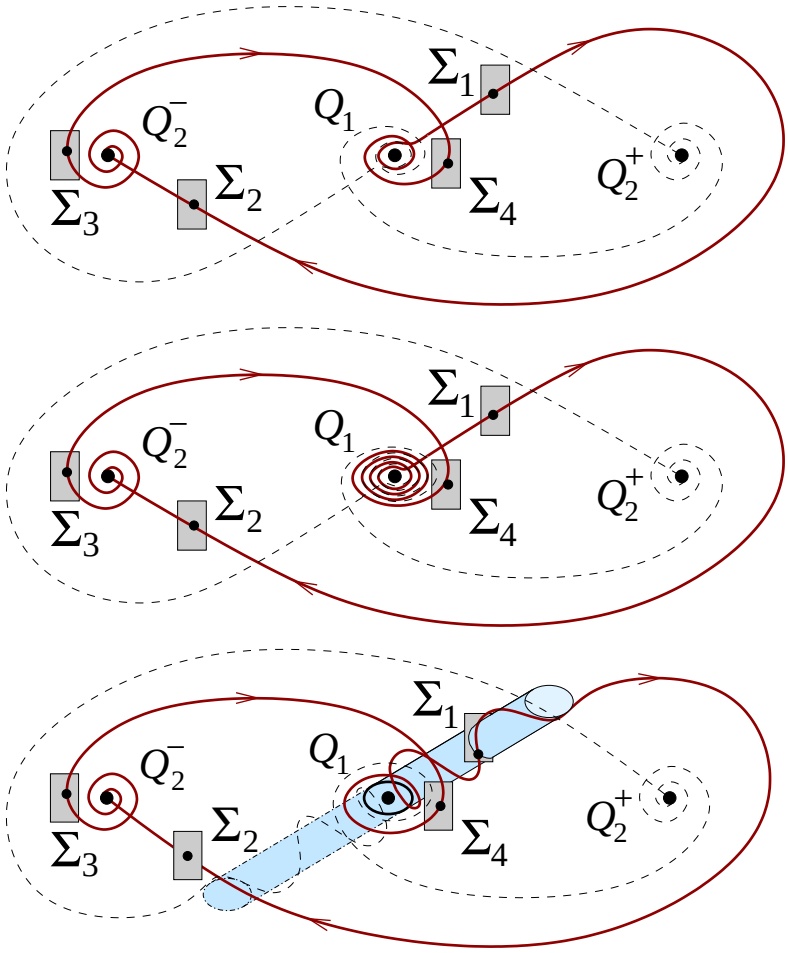

Figure 3: Schematic diagram of homoclinic connections to Q_2^-. We have also drawn the transversal sections needed in the construction of the Poincaré map and the unstable cylinder of the periodic orbit Γ (for $\mu > 0$).

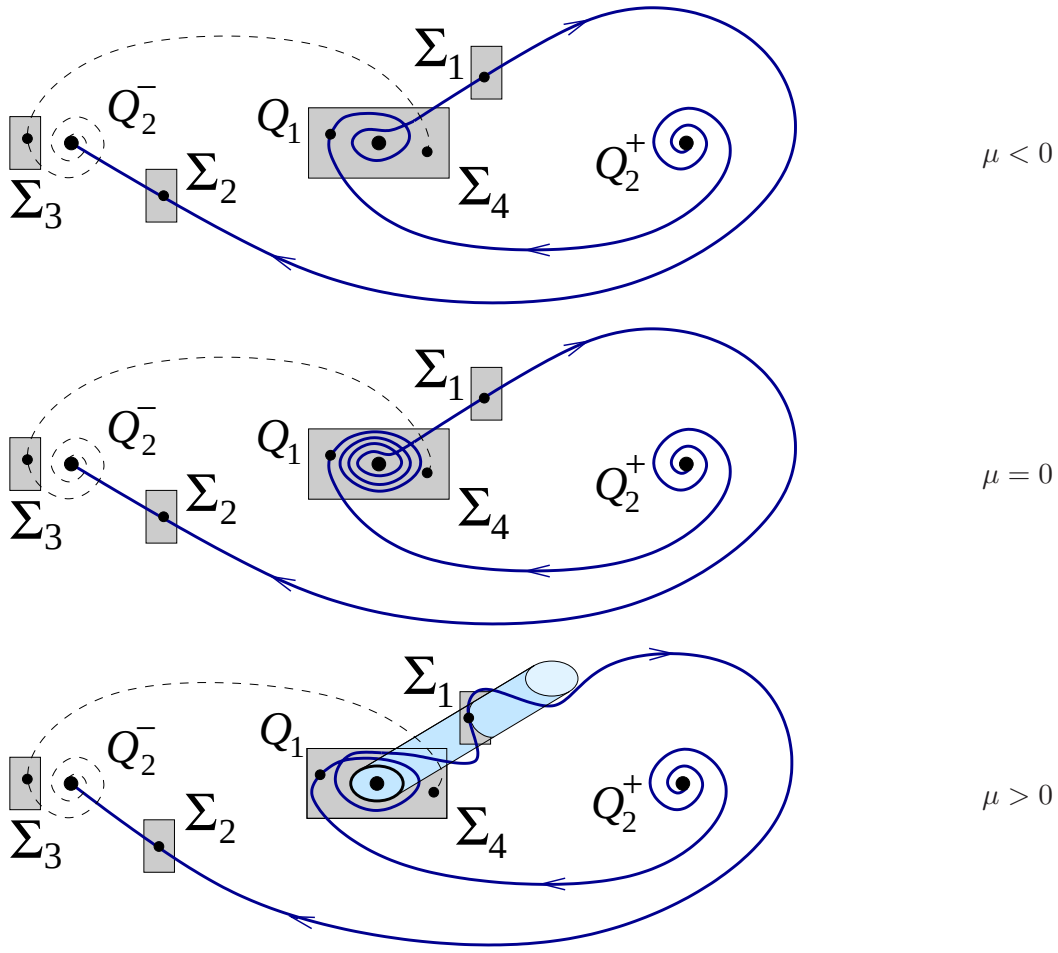

Figure 4: Heteroclinic connections from Q_2^+ to Q_2^-, depending on the value of the parameter μ. The dashed curve is the part of the symmetrical heteroclinic connection used to complete the path through the Poincaré sections.

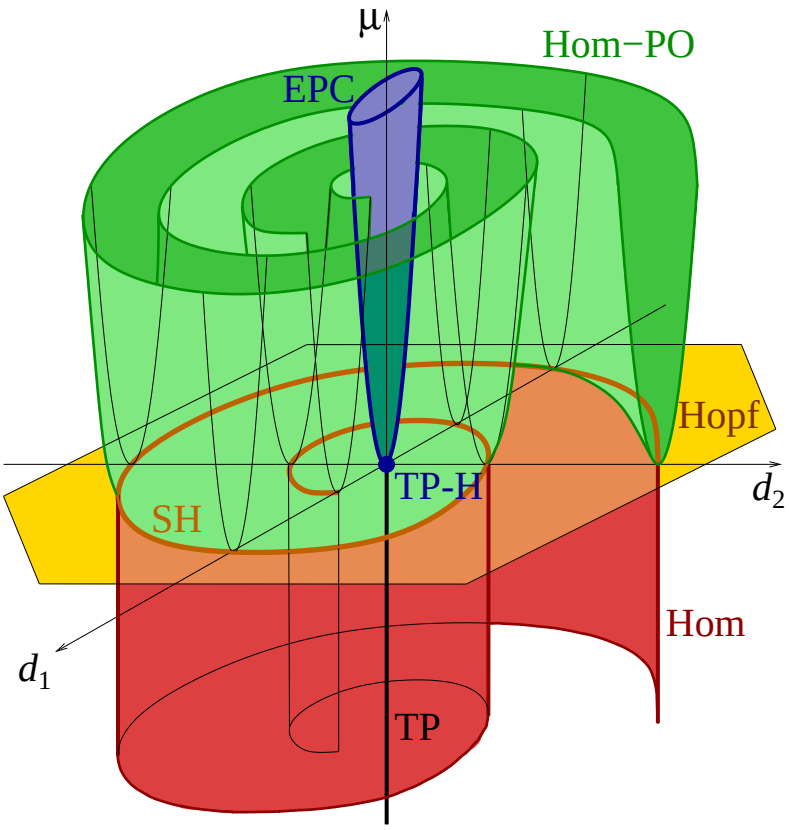

Figure 5: Location of the different kinds of heteroclinic and homoclinic connections related to Q_1 and Γ in the space of parameters (d_1, d_2, μ). The following notation is used: T–points (TP), EPC–points (EPC), T–point–Hopf (TP-H), homoclinic connections to Q_1 (Hom), homoclinic connections to Γ (Hom-PO) and Shil'nikov-Hopf points (SH). The plane $\mu = 0$ is the surface of Hopf bifurcations of the equilibrium Q_1.

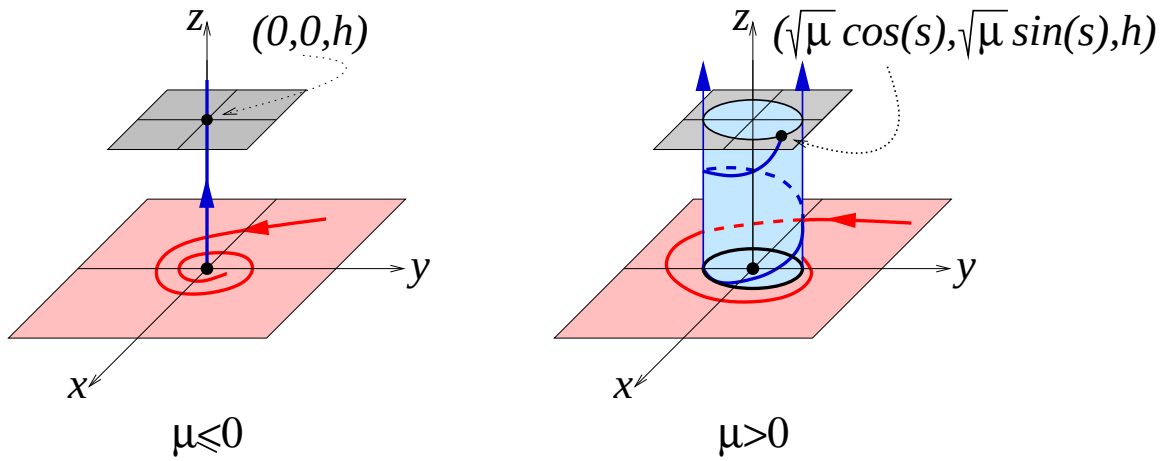

Figure 6: Configuration of the unstable manifolds of Q_1 (for $\mu \leq 0$) and Γ (for $\mu > 0$).

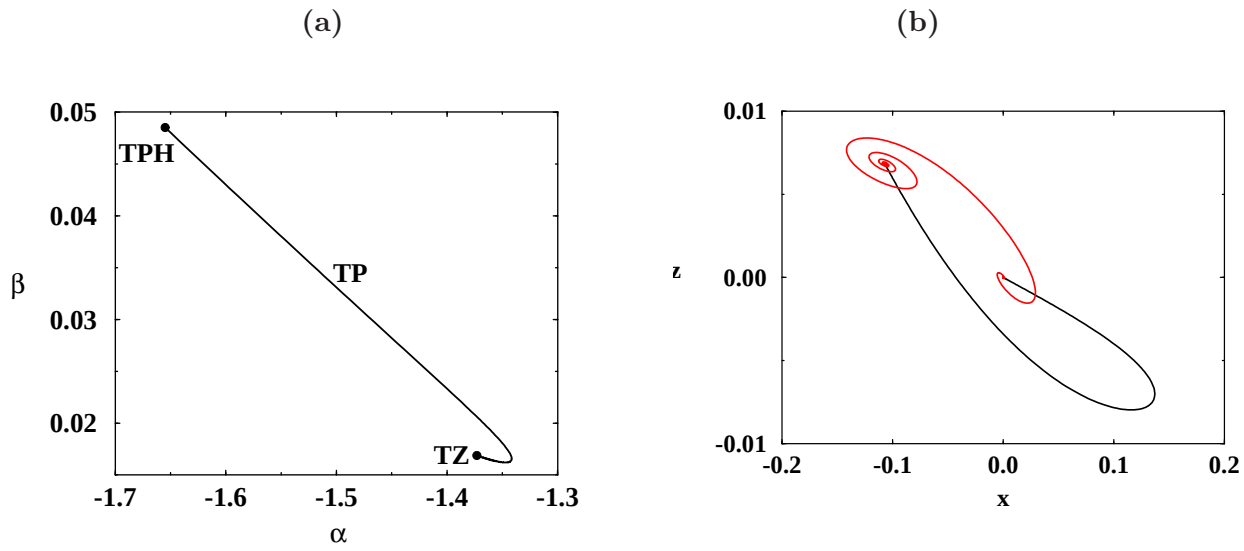

Figure 7: (a) Projection of the curve of principal T-points **TP** onto the (α, β) plane, for $\gamma = 0.3$, $a = -1$. This curve emerges from a triple-zero linear degeneracy of the origin **TZ**. (b) Projection onto the xz plane of the **TP** that occurs for $\beta \approx 0.02052$, $c \approx 0.94743$, $\alpha = -1.372126$.

(a)

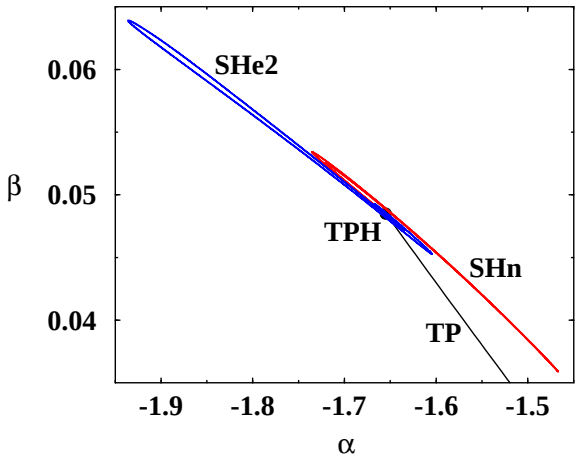

(b)

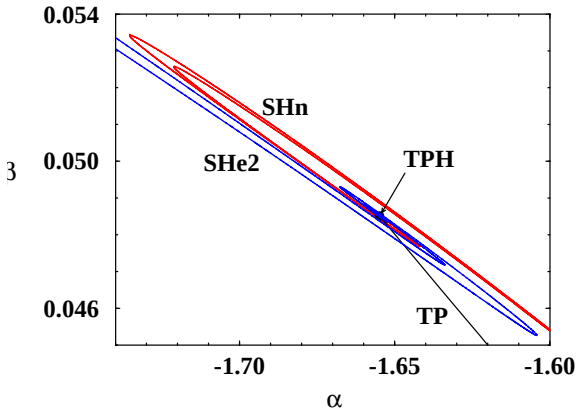

(c)

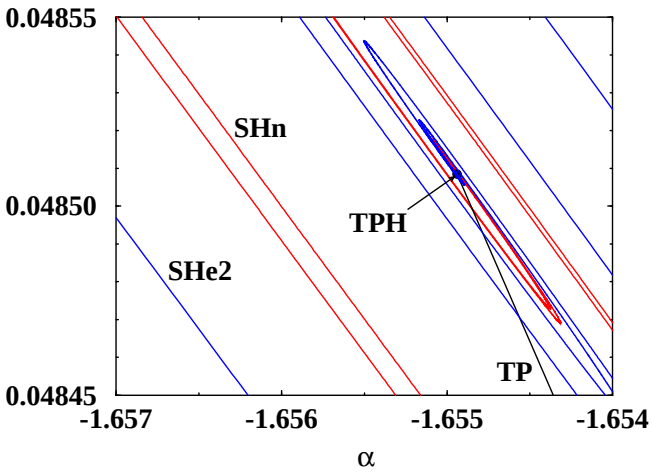

Figure 8: (a) Projection of the curves of Hopf-Shil'nikov connections onto the (α, β) plane, for $\gamma = 0.3$, $a = -1$. These curves, **SHn** and **SHe2**, bi-spiral around the T-point Hopf, **TPH**. (b) Zoom of (a). (c) Zoom of (b).

(a)

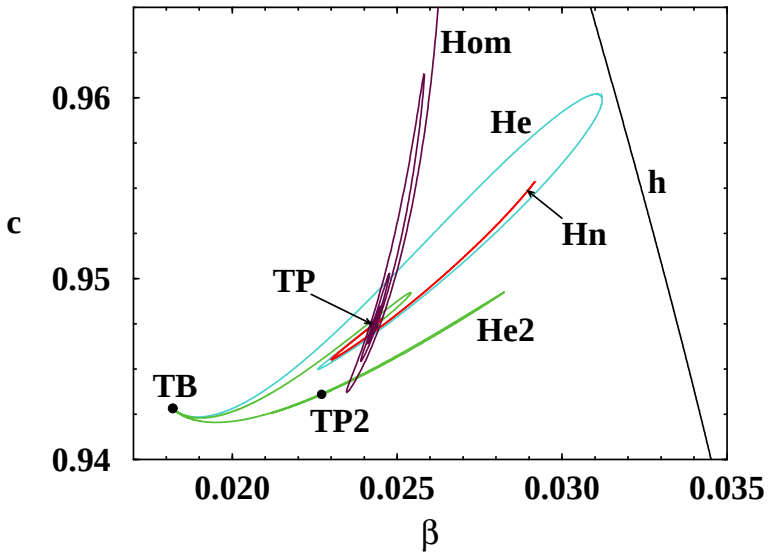

(b)

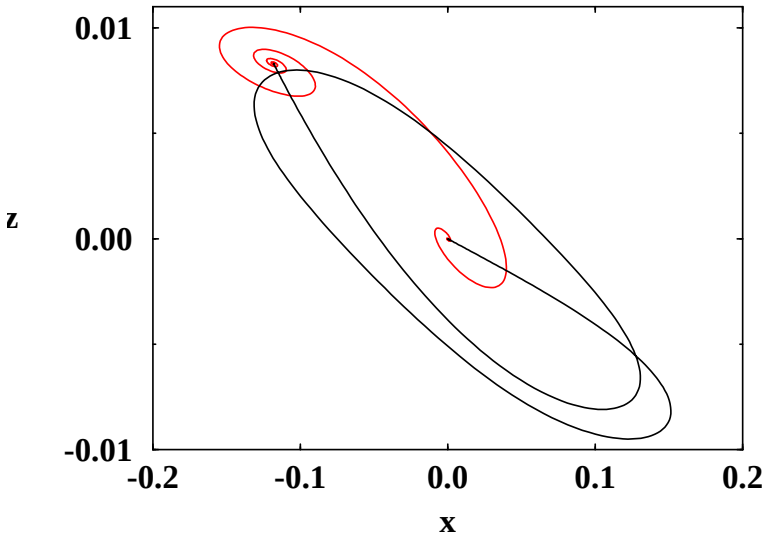

Figure 9: (a) A partial bifurcation set for $\alpha = -1.41$, $\gamma = 0.3$, $a = -1$. (b) Projection onto the xz plane of the secondary **TP2** that occurs for $\alpha = -1.41$, $\beta \approx 0.022707$, $c \approx 0.94359$.

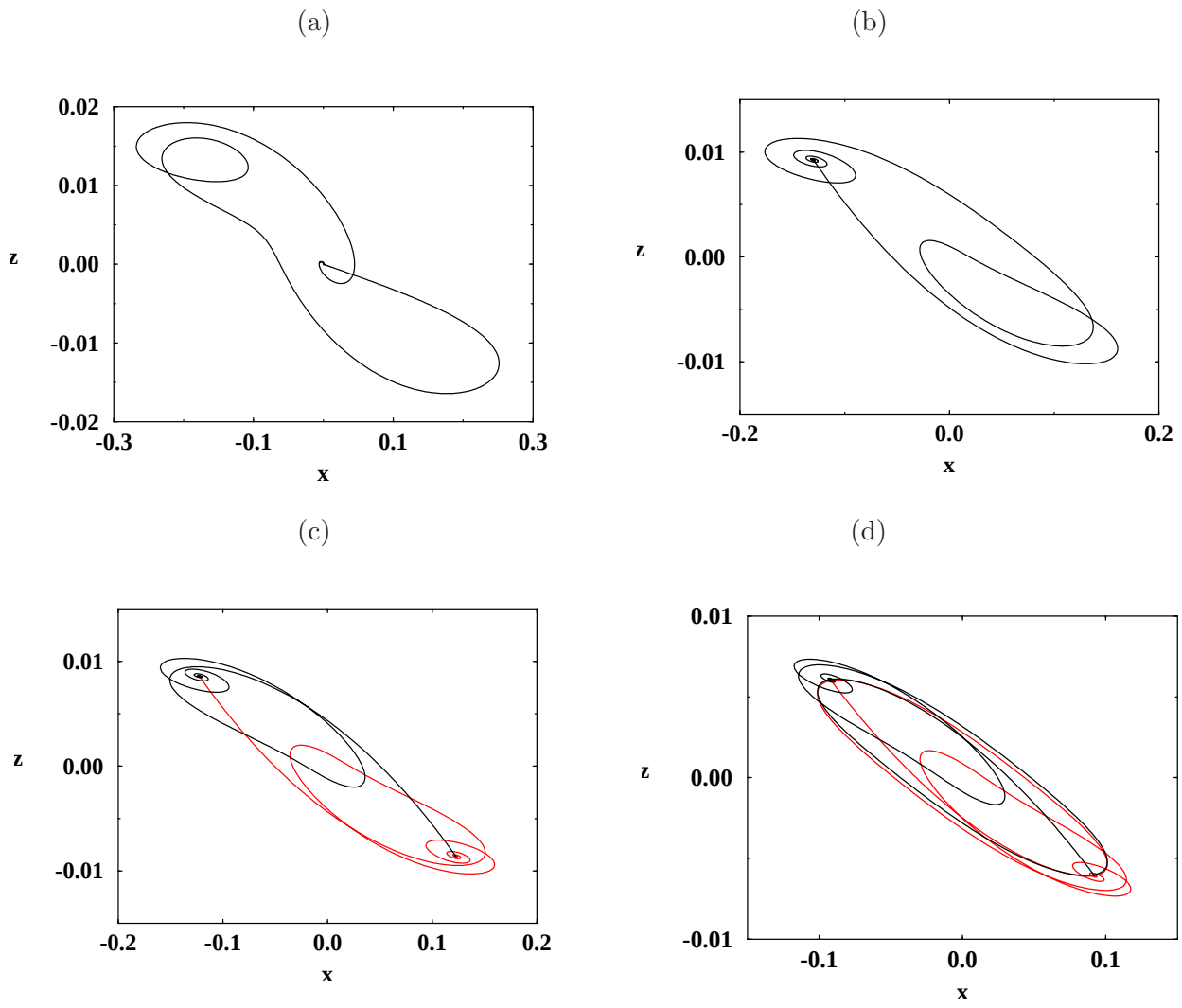

Figure 10: Projection onto the xz plane, when $\alpha = -1.41$, of: (a) a homoclinic orbit to the origin, **Hom**, for $\beta \approx 0.02597$, $c = 0.96$; (b) a homoclinic orbit to a nontrivial equilibria, **Hn**, for $\beta \approx 0.023036$, $c \approx 0.94557$; (c) a pair of heteroclinic orbits to the nontrivial equilibria, **He**, for $\beta \approx 0.022595$, $c \approx 0.94498$; (d) a pair of heteroclinic orbits to the nontrivial equilibria, **He2**, for $\beta \approx 0.021183$, $c \approx 0.94255$.

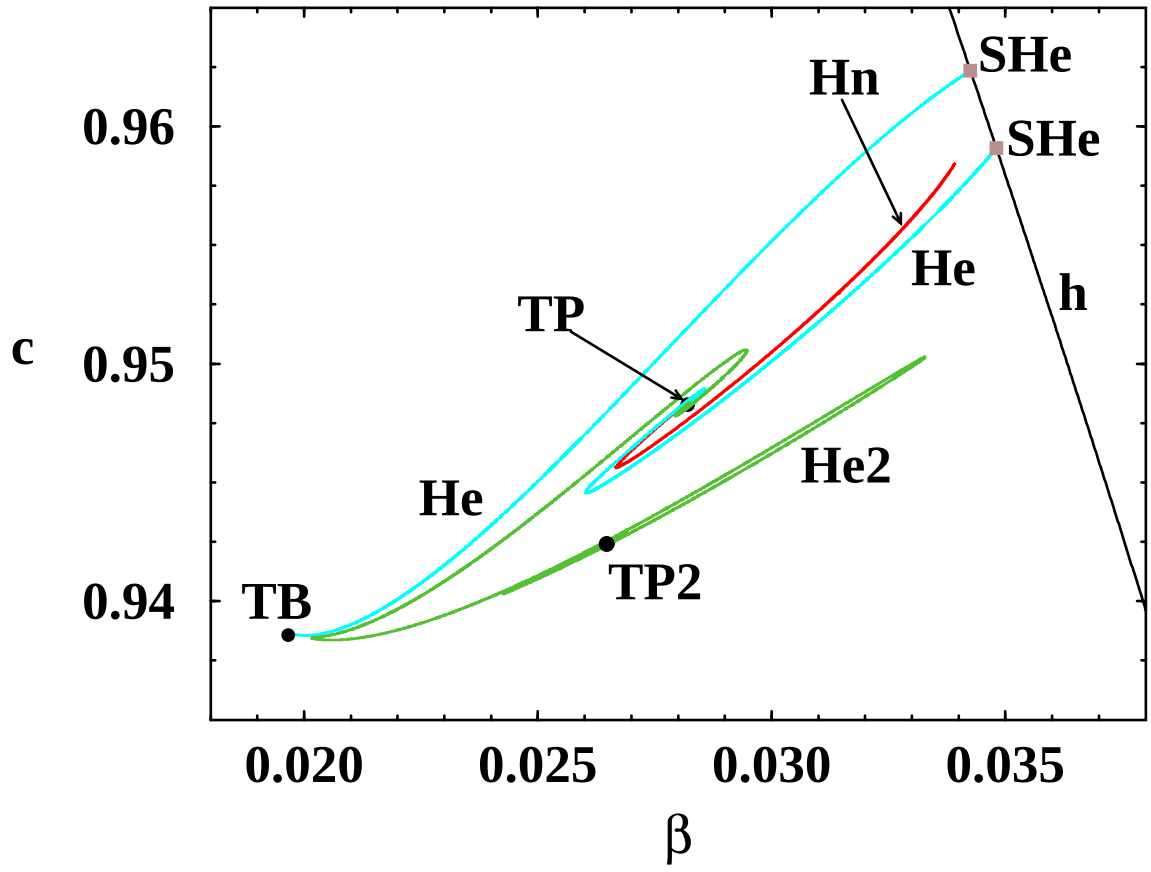

Figure 11: A partial bifurcation set for $\alpha = -1.45$, $\gamma = 0.3$, $a = -1$. Two Hopf-Shil'nikov points **SHe** of heteroclinic connections appear.

(a)

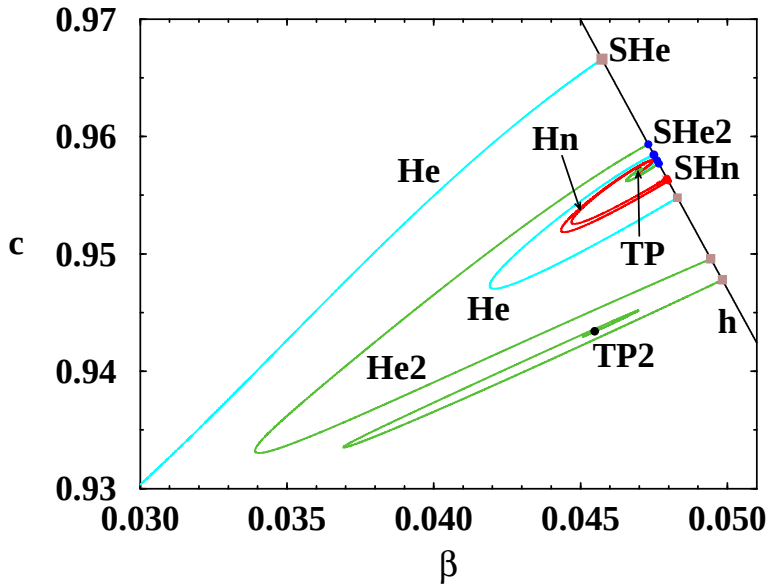

(b)

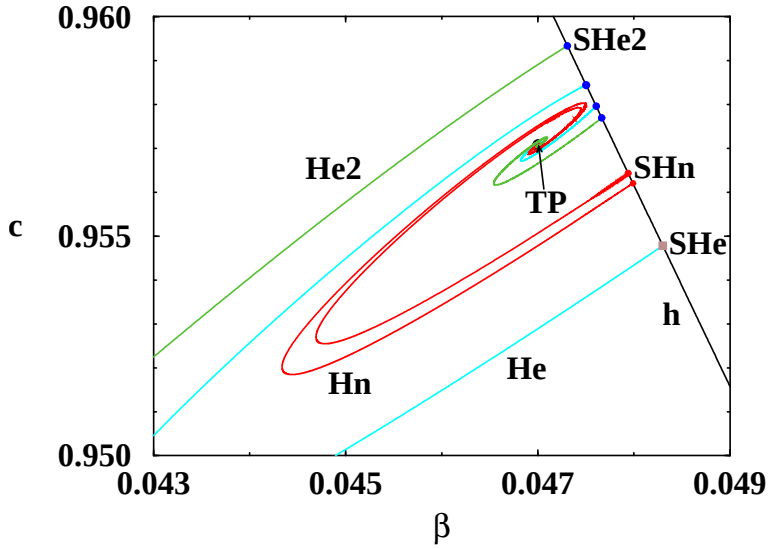

Figure 12: (a) A partial bifurcation set for $\alpha = -1.64$, $\gamma = 0.3$, $a = -1$. (b) A zoom of (a) in a neighborhood of point **TP**. Eight new Hopf-Shil'nikov points appear (4 points of curve **SHe**2, two of **SHe** and other two of **SHn**).

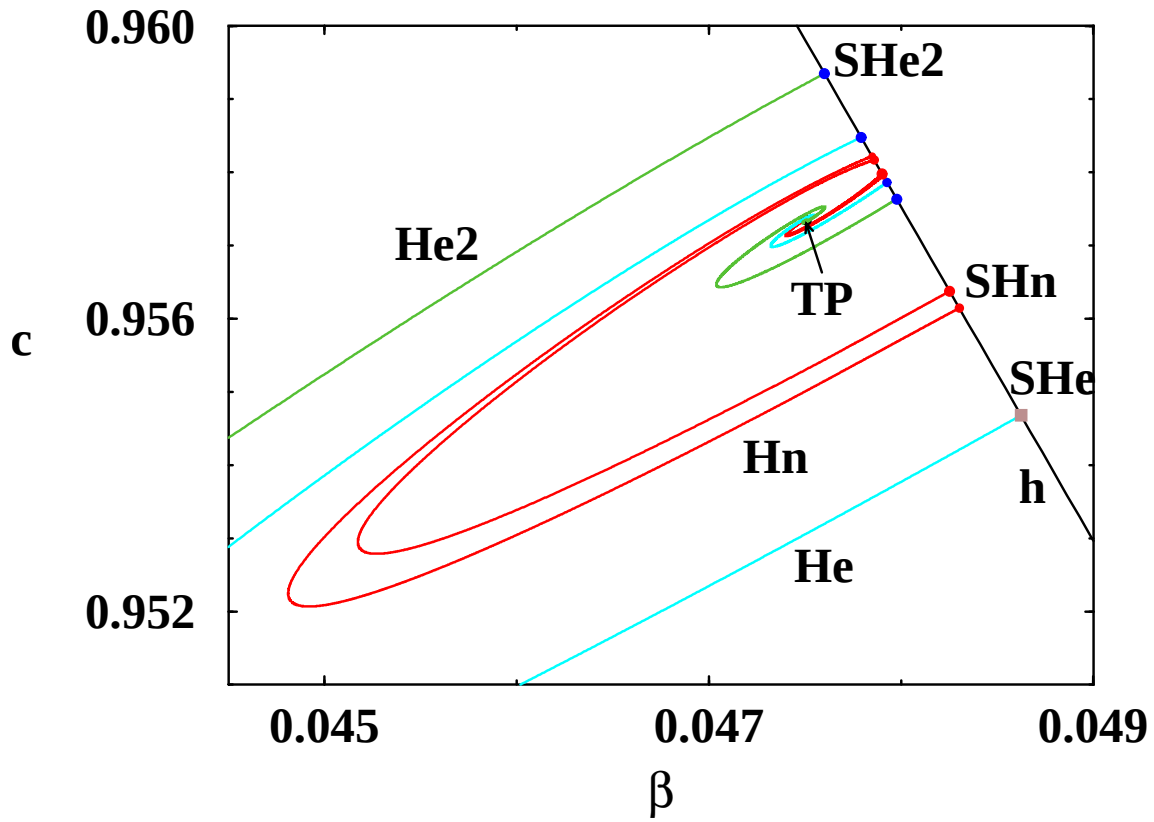

Figure 13: A partial bifurcation set for $\alpha = -1.645$, $\gamma = 0.3$, $a = -1$. Four new Hopf-Shil'nikov points **SHn** appear.

(a)

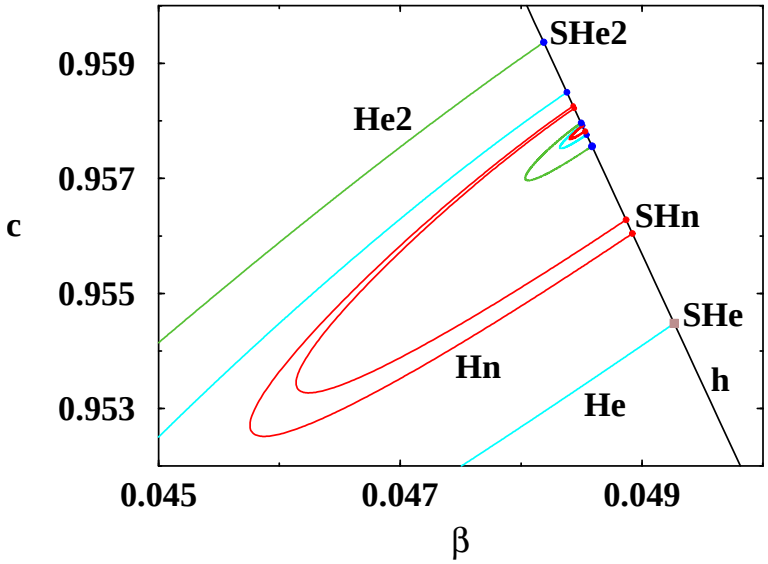

(b)

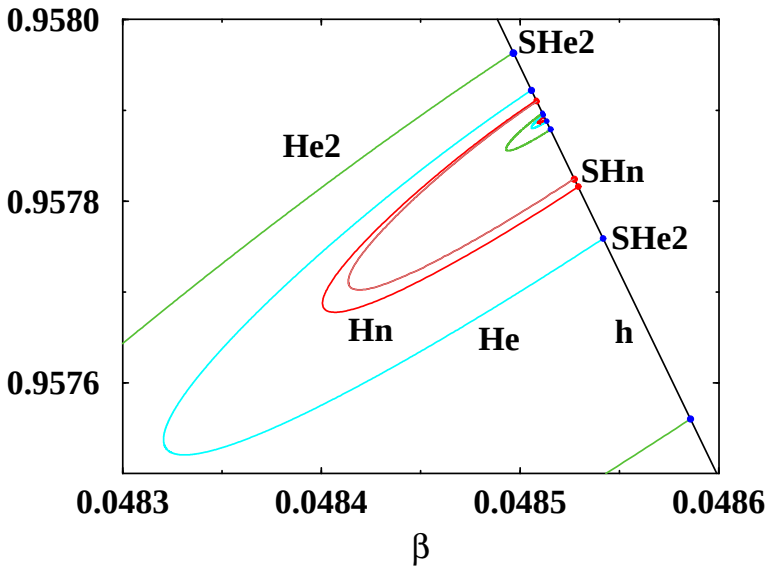

Figure 14: (a) A partial bifurcation set for $\alpha = -1.655$, $\gamma = 0.3$, $a = -1$. As we have crossed the critical value where the T-point-Hopf **TPH** occurs, no T-point appears. (b) A zoom of (a).

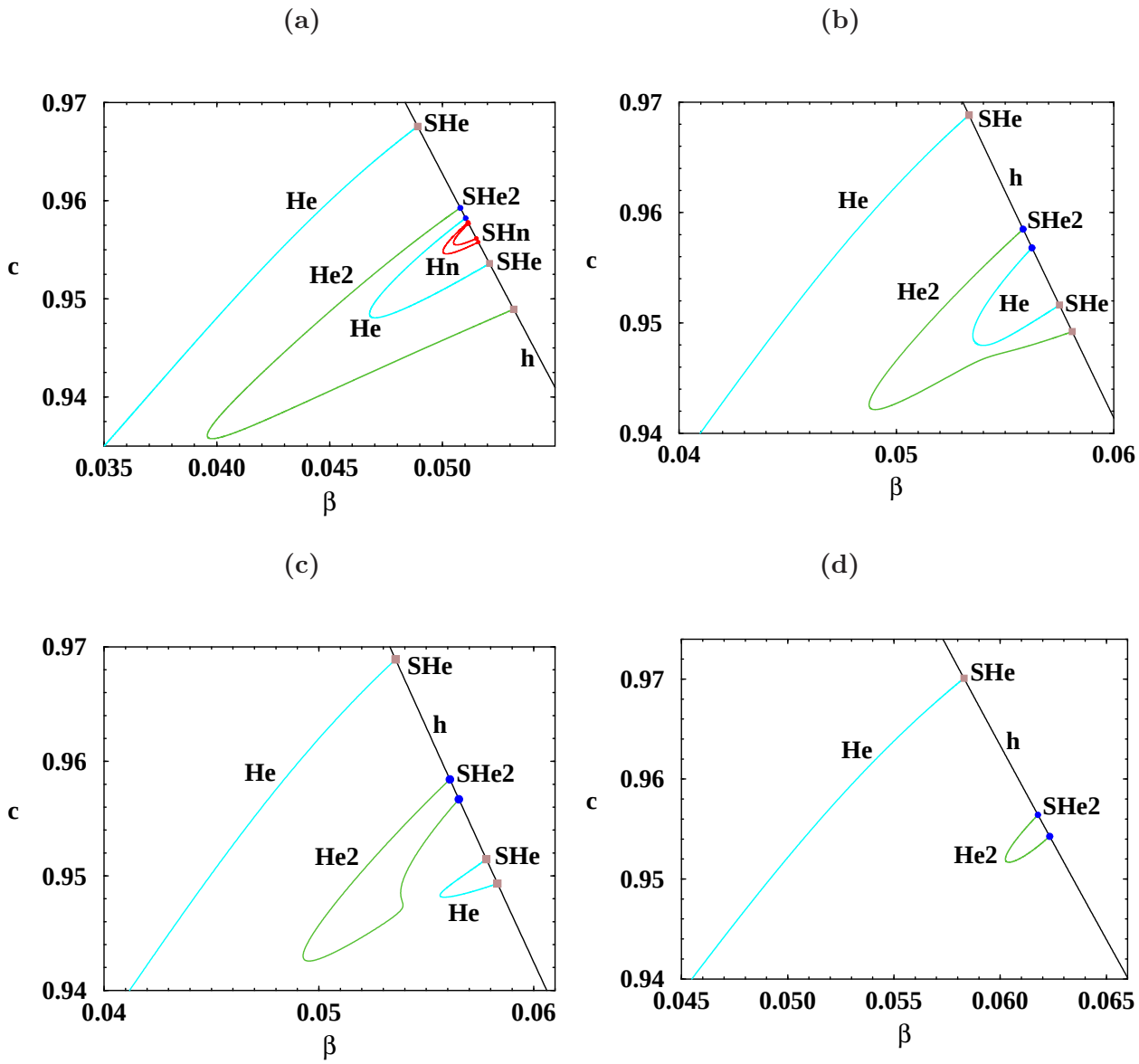

Figure 15: A partial bifurcation set for $\gamma = 0.3$, $a = -1$ and: (a) $\alpha = -1.7$; (b) $\alpha = -1.79$; (c) $\alpha = -1.795$; (d) $\alpha = -1.9$.

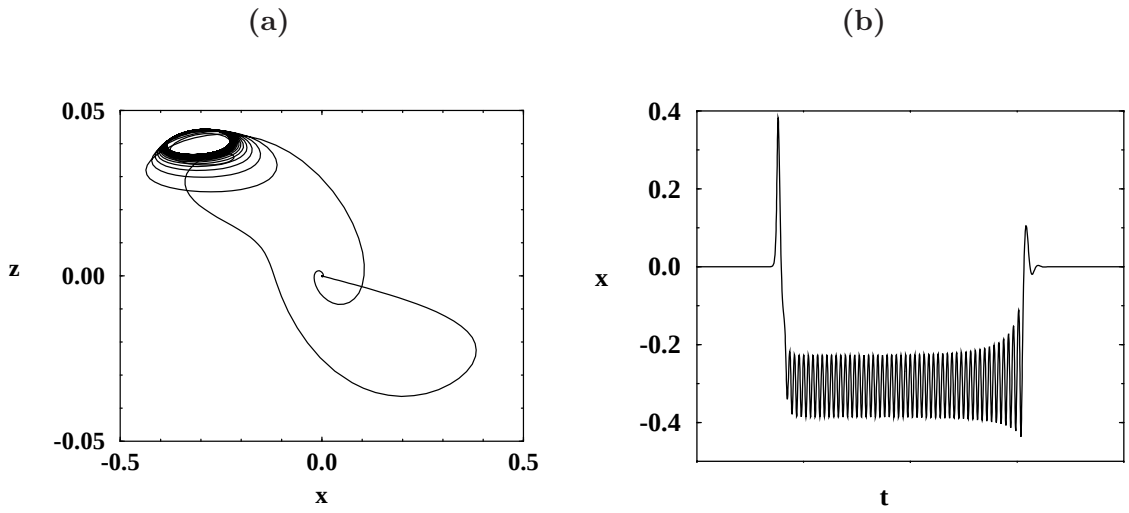

Figure 16: A homoclinic connection to the origin: (a) xz-projection; (b)temporal profile.